2009

Trichostatin A Inhibits Corneal Haze *in vitro* and *in vivo*

Ajay Sharma
Chapman University, sharma@chapman.edu

Maneesh M. Mehan
University of Missouri, Columbia

Sunilima Sinha
University of Missouri, Columbia

John W. Cowden
University of Missouri, Columbia

Rajiv R. Mohan
University of Missouri, Columbia

Recommended Citation
Sharma A, Mehan MM, Sinha S, Cowden JW, Mohan RR. Trichostatin A Inhibits Corneal Haze *in vitro* and *in vivo*. *Invest Ophthalmol Vis Sci*. 2009;50(6):2695-2701. doi:10.1167/iovs.08-2919.

Trichostatin A Inhibits Corneal Haze *in vitro* and *in vivo*

Trichostatin A Inhibits Corneal Haze In Vitro and In Vivo

Ajay Sharma,[1,2] *Maneesh M. Mehan,*[1,2] *Sunilima Sinha,*[1,2] *John W. Cowden,*[1,2] *and Rajiv R. Mohan*[1,2,3]

Purpose. Trichostatin A (TSA), a histone deacetylase inhibitor, has been shown to suppress TGF-β–induced fibrogenesis in many nonocular tissues. The authors evaluated TSA cytotoxicity and its antifibrogenic activity on TGF-β–driven fibrosis in the cornea with the use of in vitro and in vivo models.

Methods. Human corneal fibroblasts (HSFs) were used for in vitro studies, and New Zealand White rabbits were used for in vivo studies. Haze in the rabbit cornea was produced with photorefractive keratectomy (PRK) using excimer laser. Trypan blue exclusion and MTT assays evaluated TSA cytotoxicity to the cornea. Density of haze in the rabbit eye was graded with slit lamp biomicroscopy. Real-time PCR, immunoblotting, or immunocytochemistry was used to measure α-smooth muscle actin (SMA), fibronectin, and collagen type IV mRNA or protein levels. TUNEL assay was used to detect cell death.

Results. TSA concentrations of 250 nM or less were noncytotoxic and did not alter normal HSF morphology or proliferation. TGF-β1 treatment of HSF significantly increased mRNA and protein levels of SMA (9-fold), fibronectin (2.5-fold), and collagen type IV (2-fold). TSA treatment showed 60% to 75% decreases in TGF-β1–induced SMA and fibronectin mRNA levels and 1.5- to 3.0-fold decreases in protein levels but had no effect on collagen type IV mRNA or protein levels in vitro. Two-minute topical treatment of TSA on rabbit corneas subjected to -9 D PRK significantly decreased corneal haze in vivo.

Conclusions. TSA inhibits TGF-β1–induced accumulation of extracellular matrix and myofibroblast formation in the human cornea in vitro and markedly decreases haze in rabbit cornea in vivo. (*Invest Ophthalmol Vis Sci.* 2009;50:2695–2701) DOI: 10.1167/iovs.08-2919

Laser surgical procedures such as laser-assisted in situ keratomileusis (LASIK), photorefractive keratectomy (PRK), and laser epithelial keratomileusis (LASEK) are widely used for correcting refractive errors in the United States and around the world.[1–3] LASIK is the most popular procedure because it involves less pain, faster postoperative recovery, and lower wound-healing response.[4–6] Nonetheless, a significant proportion of patients experience various side effects from LASIK that raise questions about the safety of this procedure.[2,7] Recently, the United States Food and Drug Administration formed a LASIK study task force to address side effects as an outcome of LASIK.[8] Unlike LASIK, PRK does not involve corneal flap formation and, in some patients, is the procedure of choice.[9] However, complications such as postoperative pain and haze have been reported in patients receiving PRK correction for high myopia.[10,11] Mitomycin C (MMC) is increasingly used by clinicians to treat corneal haze.[12–14] The potency of MMC to inhibit corneal haze has been shown by many clinical and experimental studies.[13–15] However, multiple complications such as limbal/scleral necrosis, corneal endothelial damage, abnormal wound healing, loss of keratocytes, and endothelial damage are reported with the topical use of MMC.[16–19] We have recently shown that topical application of MMC prevents the repopulation of keratocytes and creates an acellular zone in the rabbit cornea because no keratocyte proliferation was noted even up to 6 months.[20] These reports expose the risks of using MMC to treat corneal haze in patients and encourage the development of newer pharmacologic agents that can effectively inhibit the formation of corneal haze without causing serious side effects.

Multiple in vitro and in vivo studies performed in experimental animals have significantly increased our understanding of the cellular and molecular mechanisms involved in haze development after PRK.[21,22] PRK causes an alteration in the natural conformation of extracellular matrix and changes the cellular density and phenotype of keratocytes.[21] These factors result in decreased corneal tissue transparency, commonly referred to as corneal haze or opacity.[22] The generation of corneal myofibroblasts has recently been identified as the primary biological event responsible for the formation of corneal haze.[21,23,24] Myofibroblasts are highly contractile cells with reduced transparency attributable to decreased intracellular crystallin production.[25] Various cytokines and chemokines have also been implicated as playing important roles in corneal wound healing after PRK.[26–28] Of the many cytokines shown to modulate corneal wound healing, TGF-β plays a central role in haze development.[21,29,30] It triggers the transformation of quiescent keratocytes into corneal fibroblasts and myofibroblasts.[31]It also stimulates the de novo synthesis of the extracellular matrix proteins.[32] Thus, it was hypothesized that agents with TGF-β inactivation or neutralization properties can inhibit haze development in the cornea in vivo.

TGF-β signal transduction from the cell surface to the nucleus is mediated largely by the Smad family of intracellular proteins.[30] Recent research suggests that Smad-mediated gene expression may be affected by histone acetylation.[33,34] Histone acetylation and deacetylation are regulated by opposing activities of two enzymes, histone acetylase (HAT) and histone deacetylase (HDAC). These enzymes affect gene transcription by altering chromatin structure[35] and, therefore, play a critical role in the epigenetic regulation of gene transcription.[36] The HDAC enzymes are grouped into three classes. Class I and class II HDACs are implicated in the regulation of gene transcription, but the significance of class III HDACs is still unclear.[36]

Trichostatin A (TSA), a fermentation product derived from the cultures of *Streptomyces* species, is a reversible inhibitor of class I and class II HDACs.[34,37] TSA received special attention because it inhibits HDACs in low nanomolar concentrations compared with other known HDAC inhibitors, which work at high micromolar concentrations.[37] Because of its potency, several derivatives are at various stages of clinical development to treat cancer.[36] Recent reports have demonstrated that TSA inhibits TGF-β1–mediated synthesis of collagen, α-smooth mus-

From the [1]Mason Eye Institute and the [3]College of Veterinary Medicine, University of Missouri-Columbia, Columbia, Missouri; and the [2]Harry S. Truman Memorial Veterans' Hospital, Columbia, Missouri.

Supported by National Eye Institute Grant RO1EY17294 (RRM) and by an unrestricted grant from Research to Prevent Blindness.

Submitted for publication September 21, 2008; revised December 23, 2008; accepted March 25, 2009.

Disclosure: **A. Sharma**, None; **M.M. Mehan**, None; **S. Sinha**, None; **J.W. Cowden**, None; **R.R. Mohan**, None

The publication costs of this article were defrayed in part by page charge payment. This article must therefore be marked "*advertisement*" in accordance with 18 U.S.C. §1734 solely to indicate this fact.

Corresponding author: Rajiv R. Mohan, Mason Eye Institute, EC-210, University of Missouri-Columbia, 1 Hospital Drive, Columbia, MO 65212; mohanr@health.missouri.edu.

cle actin (SMA), and myofibroblast transformation of hepatic[38] and skin fibroblasts.[39] These TSA-mediated effects are accompanied by hyperacetylation of H3 and H4 histones.[38,39] HDAC-dependent prevention of TGF-β1–mediated transformation of fibroblasts into myofibroblasts has also been confirmed using siRNA-mediated approaches and other pharmacologic inhibitors.[34] Although the exact mechanism of TSA-mediated inhibition of TGF-β effects has not been fully elucidated, TSA has been shown to increase the levels of Smad7, 5′-TG-3′-interacting factor (TGIF), and TGIF2.[34,39] Smad7 and TGIF are well documented repressors of TGF-β–mediated signal transduction. TSA has also been reported to inhibit the interaction of Smad proteins with transcription factors such as zinc finger binding protein Sp1 and p300.[40] These transcription factors, along with Smad, bind to the promoter region of TGF-β–regulated genes. Therefore, TSA-mediated inhibition of these transcription factors will abrogate TGF-β–mediated gene expression. These reports prompted us to hypothesize that suppression of TGF-β–induced profibrotic genes with trichostatin A may be a novel approach to treat or prevent PRK-induced corneal haze.

Materials and Methods

Human Corneal Fibroblast Culture

Donor human corneas were procured from an eye bank and were used in the study in accordance with the Declaration of Helsinki for the use of human tissue. Primary human corneal fibroblasts were generated from donor human corneas according to a method described previously.[41] Briefly, the cornea was washed with cell culture medium, and the epithelium and endothelium were removed by gentle scraping with a scalpel blade. Corneal stroma was cut into small pieces and incubated in a humidified CO_2 incubator at 37°C in Dulbecco's modified Eagle's medium containing 10% fetal bovine serum to obtain human corneal fibroblasts. Seventy percent confluent cultures of human corneal fibroblasts (passages 1–3) were used for experiments. For myofibroblast generation, cultures were exposed to TGF-β1 (1 ng/mL) for 7 days under serum-free conditions. TSA was used at 50 to 500 nM concentrations. TGF-β1 was purchased from R&D Systems (Minneapolis, MN), and TSA was purchased from Sigma-Aldrich (St Louis, MO).

RNA Extraction, cDNA Synthesis, and Quantitative Real-Time PCR

Total RNA from the cells was extracted with a purification kit (RNeasy kit; Qiagen Inc., Valencia, CA) and was reverse transcribed to cDNA in accordance with the manufacturer's instructions (ImProm-II Reverse Transcription system; Promega, Madison, WI). Real-time PCR was performed (iQ5 Real-Time PCR Detection System; Bio-Rad Laboratories, Hercules, CA). A 50-μL reaction mixture containing 2 μL cDNA (250 ng), 2 μL forward primer (200 nM), 2 μL reverse primer (200 nM), and 25 μL 2× green super mix (iQ SYBR; Bio-Rad Laboratories) was run at a universal cycle (95°C for 3 minutes, 40 cycles at 95°C for 30 seconds, and 60°C for 60 seconds) in accordance with the manufacturer's instructions. For SMA, the forward primer sequence TGGGTGACGAAGCACAGAGC and the reverse primer sequence CTTCAGGGGCAACACGAAGC were used. For fibronectin, the forward primer sequence was CGCAGCTTCGAGATCAGTGC, and the reverse primer sequence was TCGACGGGATCACACTTCCA. For type IV collagen, the forward primer sequence of AGGTGTTGACGGCTTACCTG and the reverse primer sequence of TTGAGTCCCGGTAGACCAAC were used for real-time PCR. β-Actin forward primer (CGGCTACAGCTTCACCACCA) and reverse primer (CGGGCAGCTCGTAGCTCTTC) were used as housekeeping genes. Cycle threshold (Ct) was used to detect the increase in the signal associated with an exponential growth of PCR product during the log-linear phase. Relative expression was calculated with $2^{-\Delta\Delta}$Ct. ΔCt validation experiments showed similar amplification efficiency for all templates used (difference between linear slopes for all templates $<$ 0.1). Three independent experiments were performed, and the average (±SEM) results are presented in graphic form.

Immunoblotting

Cells were washed with ice-cold PBS and lysed directly onto plates with RIPA protein lysis buffer containing protease inhibitor cocktail (Roche Applied Sciences, Indianapolis, IN). Samples were suspended in Laemmli denaturing sample buffer (30 μL) containing β-mercaptoethanol, vortexed for 1 minute, centrifuged for 5 minutes at 10,000*g*, and boiled at 70°C for 10 minutes. Protein samples were resolved by 4% to 10% SDS-PAGE and were transferred to a 0.45-μm pore size polyvinylidene difluoride membrane (Invitrogen, San Diego, CA). The membrane was incubated with SMA (Dako, Carpinteria, CA), fibronectin, or GAPDH primary antibodies (Santa Cruz Biotechnology Inc., Santa Cruz, CA) followed by secondary anti-mouse or anti-goat antibodies (Santa Cruz Biotechnology).

Cell Proliferation Assay

To assess the effect of TSA treatment on corneal fibroblast proliferation, the number of viable cells was counted according to an MTT-based method, as described previously.[42] The assay uses a tetrazolium compound, MTT (Sigma-Aldrich), that is bioreduced by viable cells to a purple formazan product (proportional to the number of viable cells) and can be detected by measuring absorbance at 570 nm. With the use of a 96-well plate, 2×10^3 cells/well were plated in 100 μL DMEM, and 10 μL MTT reagent was added to each well. Wells containing media alone, without cells, served as negative controls. The plates were incubated for various amounts of time at 37°C in a humidified 5% CO_2 incubator. To study the effect of TSA on cell growth, 50 to 500 nM TSA was added to each well. Absorbance was recorded at 570 nm with a 96-well plate reader (FLx 800; BioTEk, Winooski, VT).

Corneal Haze Generation and TSA Application

Twelve female New Zealand White rabbits, each weighing 2.5 to 3.0 kg, were included in this study. All animals were treated in accordance with the tenets of the ARVO Statement for the Use of Animals in Ophthalmic and Vision Research. Animals were anesthetized by intramuscular injection of ketamine hydrochloride (40 mg/kg) and xylazine hydrochloride (5 mg/kg). In addition, topical proparacaine hydrochloride 0.5% (Alcon, Fort Worth, TX) was applied to each eye just before surgery. With the animal under general and local anesthesia, a wire lid speculum was positioned, and a 7-mm diameter area of epithelium overlying the pupil was removed by scraping with a no. 64 blade (Beaver; Becton-Dickinson, Franklin Lakes, NJ). Corneal haze was induced by performing −9.0 D PRK with a 6-mm ablation zone on the central stroma with an excimer laser (Summit Apex; Alcon). Only one eye from each animal was used for the surgical procedure; the contralateral eye served as the naive control. Animals were divided into two groups consisting of control and TSA-treated animals. In the TSA-treated group, a topical 0.02% solution of TSA was applied for 2 minutes immediately after PRK, followed by copious washing with balanced salt solution (BSS; Alcon, Ltd., Ft. Worth, TX).

Biomicroscopic Grading of Corneal Haze

The level of opacity (haze) in the cornea was measured with slit lamp 4 weeks after PRK according to a method reported previously[43] with animals under general anesthesia. Grade 0 was a completely clear cornea; grade 0.5 had trace haze seen with careful oblique illumination with slit lamp biomicroscopy; grade 1 was more prominent haze not interfering with the visibility of fine iris details; grade 2 was mild obscuration of iris details; grade 3 was moderate obscuration of the iris and lens; and grade 4 was complete opacification of the stroma in the area of the ablation. Haze grading was performed in a masked manner.

Tissue Collection

Rabbits were euthanatized with overdoses of pentobarbitone (100 mg/kg) while still under ketamine/xylazine anesthesia. Corneas were removed with forceps and sharp Westcott scissors, embedded in liquid optimal cutting temperature compound (Sakura FineTek, Torrance, CA) within a 24 × 24 × 5-mm mold (Fisher, Pittsburgh, PA), and snap

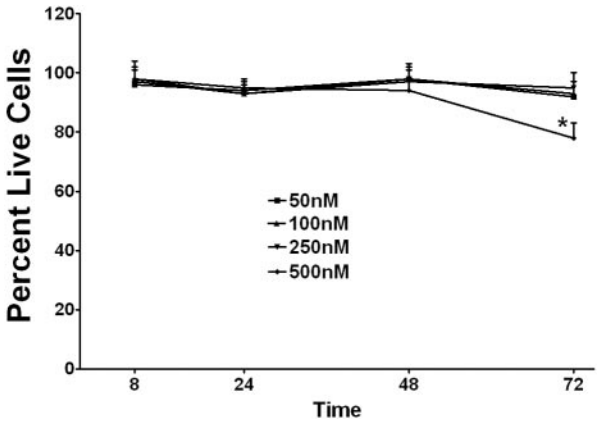

FIGURE 1. Time- and dose-dependent cytotoxicity of TSA to cultured human corneal fibroblasts. Cultures were exposed to different concentrations of TSA (50, 100, 250, 500 nM) for 72 hours, and cell viability was quantified with MTT or trypan blue assay at 8, 24, 48, or 72 hours. TSA did not produce any cytotoxic effect on the cultured fibroblasts. Data are shown as mean ± SEM of percentage live cells. $^{*}P < 0.01$ versus control.

frozen. Frozen tissue blocks were maintained at −80°C. Tissue sections (7 μm) were cut with a cryostat (CM 1850; Leica, Wetzlar, Germany) Sections were placed on 25 × 75 × 1-mm microscope slides (Superfrost Plus; Fisher, Pittsburgh, PA) and were maintained frozen at −80°C until staining was performed.

TUNEL and Immunohistochemistry Assays

For TUNEL assay, tissue sections were fixed in acetone at −20°C for 10 minutes, dried at room temperature for 5 minutes, and placed in PBS BSS. Fluorescent apoptosis detection assay (ApopTag; Chemicon International, Temecula, CA) that detects apoptosis and, to a lesser extent, necrosis was performed in accordance with the manufacturer's instructions. Positive (4 hours after mechanical corneal scrape) and negative (unwounded) control slides were included in each assay.

Immunofluorescence staining for α-SMA, a marker for myofibroblasts, was performed using mouse monoclonal antibody for SMA (catalog no. M0851; Dako, Carpinteria, CA). Tissue sections (7 μm) were incubated at room temperature with the monoclonal antibody for SMA at a 1:200 dilution in 1× PBS for 90 minutes and with secondary antibody Alexa 488 goat anti-mouse IgG (catalog no. A11001; Invitrogen) at a dilution of 1:500 for 1 hour. For collagen type IV immunostaining, rat monoclonal AbH11, AbH22 (generous gift from Nirmala Sundarraj, University of Pittsburgh, Pittsburgh, PA), and goat polyclonal antibody (catalog no. sc9302; Santa Cruz Biotechnology Inc., Santa Cruz, CA) were used at 1:100 dilutions for 2 hours. Appropriate Alexa 594 secondary antibodies (catalog nos. A-11058 and A-11007; Invitrogen) were used at a dilution of 1:500 for 1 hour. For fibronectin immunostaining, goat polyclonal primary antibody (catalog no. sc6952; Santa Cruz Biotechnology) was used. Tissues were incubated at room temperature at 1:200 dilution for 90 minutes, followed by secondary antibody Alexa 594 donkey anti-goat IgG (catalog no. A11058; Invitrogen) at a dilution of 1:500 for 1 hour. Tissues were mounted with mounting medium containing DAPI (catalog no. H1200; Vectashield; Vector Laboratories, Inc. Burlingame, CA) to visualize nuclei in the tissue sections. Irrelevant isotype-matched primary antibody, secondary antibody alone, and tissue sections from naive eyes were used as negative controls for each immunocytochemistry experiment. Sections were viewed and photographed with a fluorescence microscope (Leica) equipped with a digital camera (SpotCam RT KE; Diagnostic Instruments Inc., Sterling Heights, MI).

Quantification of SMA-Positive Cells

SMA-positive cells in six randomly selected, nonoverlapping, full-thickness central corneal columns extending from the anterior stromal surface to the posterior stromal surface were counted according to a method reported previously.[44] The diameter of each column was a 400× microscope field.

Image and Statistical Analyses

Results were expressed as mean ± SEM. Statistical analysis was performed with two-way analysis of variance (ANOVA) followed by Bonferroni multiple comparisons test for cell toxicity assay. Real-time PCR data results were analyzed with one-way ANOVA followed by Tukey multiple comparison tests. Corneal haze quantification data were analyzed with nonparametric one-way ANOVA with Wilcoxon rank sum test. $P < 0.05$ was considered significant. Gel data were analyzed with ImageJ 1.38 X image analysis software (developed by Wayne Rasband, National Institutes of Health, Bethesda, MD; available at http://rsb.info.nih.gov/ij/index.html).

RESULTS

Effect of TSA on Cell Viability

To assess any potential toxicity of TSA treatment, we evaluated the time-dependent effect of four different concentrations of TSA on cell viability with the use of cultured human corneal fibroblasts. As seen in Figure 1, of the four tested concentrations of TSA, three (50, 100, 250 nM) had no significant effect on the percentage of live cells up to the tested time point of 72 hours. TSA caused a decrease in the live cell count only at the 500-nM dose (18% $P < 0.01$) at 72 hours (Fig. 1).

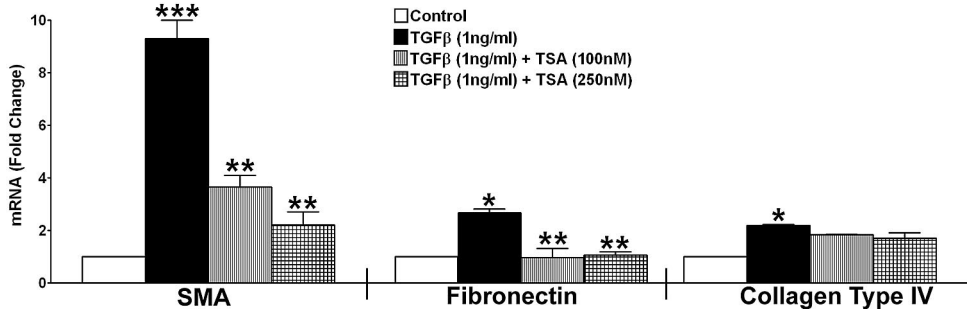

FIGURE 2. Real-time quantitative PCR showing differential change in SMA (*left*), fibronectin (*middle*), and collagen type IV (*right*) expression in human corneal fibroblast cultures exposed to TGF-β1 (1 ng/mL) for 7 days under serum-free conditions with or without TSA. TGF-β1 caused a 9-fold increase in SMA, a 2.5-fold increase in fibronectin, and a 2-fold increase in collagen type IV levels. TSA treatment inhibited TGF-β1–induced SMA and fibronectin expression significantly. $^{*}P < 0.01$ versus control; $^{**}P < 0.01$ versus TGF-β1 treatment; $^{***}P < 0.001$ versus control.

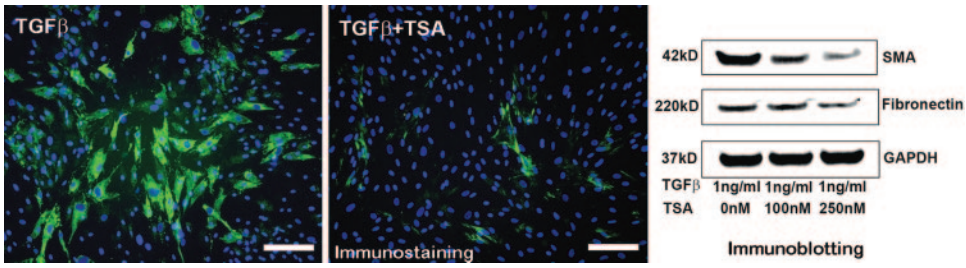

FIGURE 3. Immunocytochemistry (*left, middle*) and immunoblotting (*right*) analyses showed significant decreases in myofibroblast formation by TSA in corneal fibroblast cultures grown in the presence of TGF-β1 (1 ng/mL) under serum-free conditions. Cell nuclei are stained *blue* with DAPI, and SMA-positive cells are stained *green*. Equal quantity of protein was loaded in each lane. GAPDH was used as a housekeeping gene. TSA treatment showed a significant 3-fold decrease in SMA and a 1.5-fold decrease in fibronectin expression. Scale bar, 100 μm.

Effect of TSA Treatment on TGF-β1–Mediated Myofibroblast Generation in Cultured Human Corneal Fibroblasts

We quantified mRNA and protein levels of α-SMA, a marker of myofibroblasts, in human corneal fibroblasts with real-time PCR, Western blotting, and immunohistochemistry. TGF-β1 treatment of cultured human corneal fibroblasts resulted in a 9-fold increase ($P < 0.001$) in SMA mRNA levels. TSA treatment of cultured human corneal fibroblasts at 100 and 250 nM caused 60% ($P < 0.01$) and 75% ($P < 0.01$) reductions, respectively, in TGF-β1–mediated increased levels of SMA (Fig. 2). Western blot analysis of TGF-β1–treated human corneal fibroblasts revealed a significant increase in protein levels of SMA. Trichostatin treatment caused 2-fold (100-nM dose) and 3-fold (250-nM dose) decreases in TGF-β1–induced levels of SMA (Fig. 3). These results were further complemented by SMA immunohistochemical staining, demonstrating a significant decrease in SMA-stained cells in TSA-treated human corneal fibroblasts (Fig. 3) compared with TGF-β1–treated controls.

Effect of TSA Treatment on TGF-β1–Mediated Alteration of Extracellular Matrix Proteins in Cultured Human Corneal Fibroblasts

To evaluate the effect of TSA treatment on TGF-β1–induced alterations of extracellular matrix proteins, we quantified mRNA and protein levels of fibronectin and collagen type IV using real-time PCR and Western blotting. TGF-β1 treatment of cultured human corneal fibroblasts caused a 2.5-fold increase ($P < 0.01$) in fibronectin mRNA level (Fig. 2). Additionally, TGF-β1 also caused a significant increase in fibronectin protein level, as quantified by Western blot analysis. TSA (100 nM, 250 nM) treatment of these corneal fibroblasts caused a 60% to 64% ($P < 0.01$) reduction in TGF-β1–mediated increased levels of fibronectin mRNA and a 1.5-fold (250-nM dose) decrease in TGF-β1–mediated increased levels of fibronectin protein levels (Fig. 3).

TGF-β1 stimulation of cultured human corneal fibroblasts resulted in a 2-fold increase ($P < 0.01$) in collagen type IV mRNA as revealed by real-time PCR. TSA treatment of these TGF-β1–treated HSFs did not cause any significant change in collagen type IV mRNA levels (Fig. 2).

Slit Lamp Biomicroscopy Evaluation of TSA Treatment on PRK-Induced Corneal Haze

Corneal haze was evaluated with slit lamp biomicroscopy 4 weeks after −9 D PRK. The 4-week point was chosen based on the results of our previous studies in which we noticed peak corneal haze at this time.[20,22,44] Control corneas subjected to −9 D PRK had an average haze of 3.5 on the Fantes scale. Topical application of TSA (0.02% for 2 minutes) caused a statistically significant decrease ($P < 0.01$) in corneal haze, with an average score of 1 on the Fantes scale (Fig. 4B). No corneal haze was noted in untreated control corneas, which were not subjected to PRK treatment (Fig. 4A).

Effect of TSA Treatment on PRK-Induced Myofibroblast Generation in Rabbit Corneas

The formation of haze in rabbit corneas was also confirmed by the immunocytochemical detection of myofibroblasts (Figs. 5A, 5B) and quantification of SMA-positive cells in tissue sections. No SMA-positive cells were observed in untreated control corneas. In contrast, rabbit corneas collected 4 weeks after −9 D PRK demonstrated high numbers of SMA-positive myofibroblast cells, mostly in the anterior stroma below the epithelium. Two-minute topical TSA application immediately after PRK significantly (60%; $P < 0.01$) reduced the number of SMA-positive cells in the rabbit stroma (Fig. 6).

Effect of TSA Treatment on PRK-Induced Alteration of Extracellular Matrix Proteins in Rabbit Corneas

Immunohistochemical staining for fibronectin was noted in the stromas of the rabbit corneas subjected to −9 D PRK. Fibronectin expression was confined to the zone of laser photoablation,

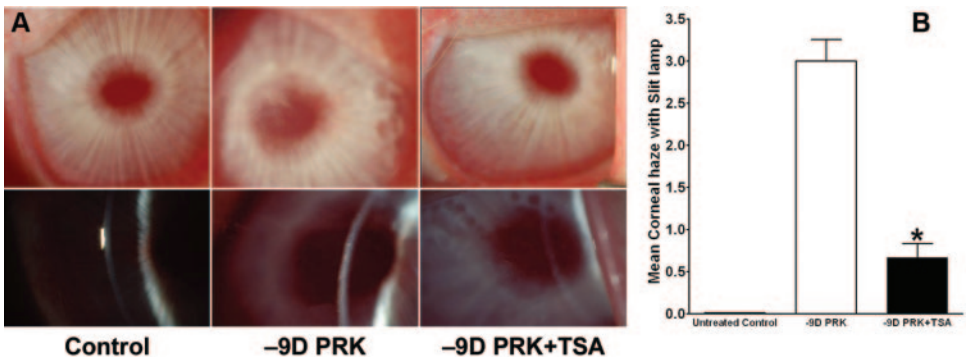

FIGURE 4. (**A**) Representative slit lamp microscopy images demonstrating density and location of haze in control (*left*), PRK-treated (*right*), and PRK+0.02% TSA–treated (*middle*) rabbit corneas. (**B**) Biomicroscopic quantification of corneal haze. A significant decrease in corneal haze was observed in TSA-treated corneas ($P < 0.01$).

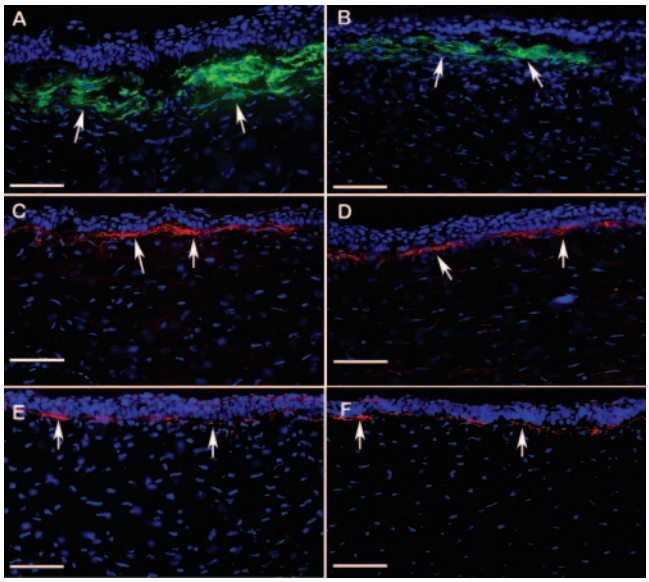

FIGURE 5. Representative immunohistochemistry images of corneal tissue sections showing levels of SMA (**A**, **B**), fibronectin (**C**, **D**), and collagen type IV (**E**, **F**) in rabbit corneas collected 4 weeks after −9 D PRK with or without TSA application. DAPI-stained nuclei are shown in *blue*, SMA-stained cells are shown in *green*, and fibronectin or collagen type IV-positive cells are shown in *red*. TSA-treated corneas showed significant decreases in SMA (**B**; $P < 0.01$) and notable decreases in fibronectin levels in the stroma compared with control corneas (**A**, **C**). No significant change was noted in collagen type IV (**E**, **F**). *Arrows*: positive protein immunostaining. Scale bar, 100 μm.

with a sharp demarcation between ablated and nonablated zones. In the ablated zone positively stained for SMA, fibronectin expression was noted in the anterior stroma, and it colocalized around SMA-positive cells. In the rest of the anterior stroma, which did not stain for SMA, fibronectin distribution was observed only around the area of basement membrane, just below the epithelium. TSA treatment markedly decreased fibronectin expression in the anterior stroma of PRK-treated rabbit corneas (Figs. 5C, 5D).

Immunohistochemical staining for collagen type IV performed with rat monoclonal antibodies detected collagen type IV α1 (Figs. 5E, 5F) and α2 subtypes (data not shown) in rabbit corneal epithelial basement membrane. However, immunostaining performed with a commercial antibody (sc9302; Santa Cruz Biotechnology) detected collagen type IV α5 expression in the stroma but was unable to recognize collagen type IV α1 in epithelial basement membrane (data not shown). None of the collagen immunohistochemistry experiments showed appreciable changes in collagen type IV levels in the PRK-treated rabbit corneas, with or without TSA application (Figs. 5E, 5F).

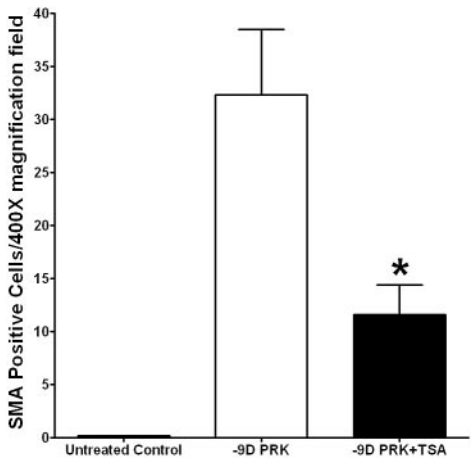

FIGURE 6. Quantification of SMA-positive cells/400× column in the tissue section obtained from rabbit corneas that underwent −9 D PRK with or without topical application of 0.02% TSA. TSA treatment decreased SMA-positive cells by 60% ($P < 0.01$).

Effect of TSA on Cell Death in Rabbit Corneas Subjected to −9 D PRK

We further evaluated the effect of TSA treatment on cell death using TUNEL assay. Few TUNEL-positive cells were noted in the stroma and epithelium in control corneas subjected to −9 D PRK (Fig. 7). Topical application of TSA in corneas subjected to −9 D PRK caused no further change in TUNEL-positive cells in stroma or epithelium. To examine any change in keratocyte density attributed to cell death caused by TSA, we compared the number of DAPI-stained nuclei in the sections obtained from rabbit corneas subjected to −9 D PRK followed by 2-minute topical application of 0.02% TSA or no TSA. No significant difference in keratocyte cell density was observed in TSA-treated or control corneas subjected to −9 D PRK, suggesting that TSA application did not cause cell death (data not shown).

DISCUSSION

Corneal haze is a common complication of PRK.[10,13,15] Corneal wound healing response to refractive surgery is proposed as the underlying mechanism for haze formation.[45,46] Therefore, attention has been focused on the use of therapeutic agents to modulate postoperative wound healing. MMC is a DNA-alkylating agent and is widely used intraoperatively by clinicians for the prevention of PRK-induced corneal haze.[12–15] Although MMC is effective in controlling haze, there are safety concerns because of several complications reported with its topical use, such as limbal/scleral necrosis, corneal endothelial damage, abnormal wound healing, and loss of keratocytes.[16–19] Thus, there is a need for safer therapeutic agents to treat corneal haze. In the present study, we demonstrate that TSA has an antifibrogenic effect in cultured human corneal fibroblasts exposed to TGF-β1 and prevents corneal haze in vivo in rabbit corneas subjected to −9 D PRK.

TSA is a potent and reversible HDAC inhibitor.[37] HDAC and HAT are key enzymes that regulate the acetylation of histone proteins.[36] Histones are core proteins around which DNA is coiled to form a compact chromatin structure. Acetylation of histone proteins causes the chromatin structure to uncoil, making it more accessible to transcription factors.[35] Accumulating evidence suggests that histone acetylation by HDAC enzymes plays a critical role in the regulation of gene transcription, and pharmacologic inhibitors of HDAC such as TSA have been used to modulate gene expression in a variety of disease conditions (cancer,[36] lupus,[47] cardiac hypertrophy,[48] spinal

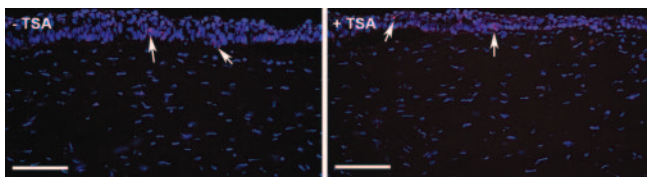

FIGURE 7. TUNEL assay of the central cornea from rabbits that underwent −9 D PRK with or without topical application of 0.02% TSA. Nuclei are stained *blue* with DAPI. Few TUNEL-positive cells (*red*) were seen in the epithelium. No loss of keratocytes (*blue*-stained nuclei) was noted in TSA-treated versus control (no TSA) rabbit corneas collected 4 weeks after −9 D PRK. *Arrows*: TUNEL-positive cells. Scale bar, 100 μm.

muscular dystrophy).[49] The initial evidence that TSA has antifibrotic effects came from studies by Rombouts et al.,[38] who demonstrated that TSA caused a significant decrease in the expression of profibrotic genes such SMA, collagen type I, and collagen type III in cultured hepatic stellate cells because of the hyperacetylation of histone H4.[38] Several of these profibrotic genes have a TGF-β response element in their promoter region.[50,51] Jester et al.[31] demonstrated that the incubation of corneal fibroblasts with TGF-β transforms them into myofibroblasts and causes increased expression of profibrotic genes such as extracellular matrix proteins and cytoskeletal proteins such as collagen, fibronectin, and SMA. A recent report has demonstrated that silencing of HDAC4 with siRNA prevents TGF-β–mediated transformation of skin fibroblasts into myofibroblasts,[34] thereby directly implicating HDAC in TGF-β–mediated fibrosis.[34] These studies led us to propose that HDAC inhibitors may block or prevent the TGF-β–mediated transdifferentiation of corneal fibroblasts into myofibroblasts. We tested this hypothesis with cultured human corneal fibroblasts and showed that TSA (a potent HDAC inhibitor) prevents TGF-β1–mediated transformation of corneal fibroblasts into myofibroblasts and significantly decreases TGF-β1–induced gene expression of SMA and fibronectin.

The precise mechanism through which TSA blocks TGF-β1–mediated gene expression has not yet been completely elucidated. However, three potential mechanisms have been proposed. First, TSA-induced hyperacetylation directly inhibits the expression of some of the TGF-β–regulated genes such as procollagen α type III and SMA.[38–40] Second, TSA increases the expression of Smad7 and TGIF proteins. These proteins are suggested to be involved in blocking Smad signaling, affecting some other genes such as procollagen α type I.[34,39] Third, TSA affects the expression of transcription factors such as p300/CBP, which act as cofactors in TGF-β-Smad–mediated gene expression.[40] Nonetheless, not all the genes activated by TGF-β are blocked by TSA, and the expression levels of some genes, such as collagen type IV[38] and PAI-1, remain unaffected.[40] We observed that in corneal fibroblasts, TSA decreased TGF-β1–induced gene expression of fibronectin and SMA but did not alter the expression of collagen type IV. These observations suggest that HDAC inhibitors may not affect global gene expression in human corneal fibroblasts. Earlier studies using cultured lymphocytes confirmed that TSA affects only approximately 2% of the cellular genes, as shown by differential gene display experiments.[52] Future studies will investigate the molecular basis of the selectivity of TSA-mediated gene expression in cornea.

The formation of corneal haze involves the apoptosis of keratocytes and the proliferation and transformation of fibroblasts into myofibroblasts.[53] These cellular changes are accompanied by SMA expression and the deposition of disorganized extracellular matrix proteins that are primarily responsible for corneal fibrosis and opacity.[21,45] Multiple studies show that TGF-β mRNA and its receptors are upregulated after PRK.[54,55] Jester et al.[56] have demonstrated the prevention of PRK-induced haze in experimental animals with the use of anti–TGF-β antibodies. Antisense approaches targeted to neutralizing TGF-β further confirm its involvement in ocular fibrosis.[57] These reports implicate the role of TGF-β in PRK-induced corneal haze. Several in vitro reports demonstrate that the biological effects of TGF-β can be blocked by TSA. Our cell culture experiments performed with TSA showed that TSA prevents the TGF-β1–induced transformation of corneal fibroblasts into myofibroblasts. Thus, we tested the effect of TSA in an in vivo rabbit model of PRK-induced corneal haze. We found that a single 2-minute application of 0.02% TSA immediately after PRK markedly reduces laser-induced corneal haze in rabbit eyes. Slit lamp biomicroscopy experiments show that TSA markedly decreases corneal opacity. Immunohistochemistry analysis revealed a decrease in the expression of α-SMA, a marker of myofibroblast formation and fibronectin, but no change in collagen expression. Based on our in vitro experiment results and our earlier experience with MMC, a single 0.02% dose of TSA was tested in this study. Further studies are needed to define the optimal dose of TSA showing minimal toxicity and maximal therapeutic effect. Although TSA is not approved for use in humans, vorinostat, a TSA structural derivative, is already in clinical use for the treatment of T-cell lymphoma,[58] and our study opens up the possibility of testing HDAC inhibitors in ophthalmology for clinical use.

Acknowledgments

The authors thank the Heartland Eye Bank (St. Louis, MO) for donor human corneas, Bill Hutchings (Alcon Refractive, Fort Worth, TX) for laser cards, and Frank G. Rieger and Chuck Hamm for help with slit lamp biomicroscopy.

References

1. Fong CS. Refractive surgery: the future of perfect vision? *Singapore Med J.* 2007;48:709–718.
2. Melki SA, Azar DT. LASIK complications: etiology, management, and prevention. *Surv Ophthalmol.* 2001;46:95–116.
3. McDonnell PJ. Emergence of refractive surgery. *Arch Ophthalmol.* 2000;118:1119–11120.
4. Shortt AJ, Bunce C, Allan BD. Evidence for superior efficacy and safety of LASIK over photorefractive keratectomy for correction of myopia. *Ophthalmology.* 2006;113:1897–1908.
5. Lee JB, Kim JS, Choe C, Seong GJ, Kim EK. Comparison of two procedures: photorefractive keratectomy versus laser in situ keratomileusis for low to moderate myopia. *Jpn J Ophthalmol.* 2001; 45:487–491.
6. El-Maghraby A, Salah T, Waring GO 3rd, Klyce S, Ibrahim O. Randomized bilateral comparison of excimer laser in situ keratomileusis and photorefractive keratectomy for 2.50 to 8.00 diopters of myopia. *Ophthalmology.* 1999;106:447–457.
7. Gimbel HV, Penno EE, van Westenbrugge JA, Ferensowicz M, Furlong MT. Incidence and management of intraoperative and early postoperative complications in 1000 consecutive laser in situ keratomileusis cases. *Ophthalmology.* 1998;105:1839–1847.
8. Schallhorn SC. Identifying potentially unhappy LASIK patients. *Cataract Refract Surg Today.* 2008;55–56.
9. Rajan MS, Jaycock P, O'Brart D, Nystrom HH, Marshall J. A long-term study of photorefractive keratectomy; 12-year follow-up. *Ophthalmology.* 2004;111:1813–1824.
10. Verma S, Corbett MC, Patmore A, Heacock G, Marshall J. A comparative study of the duration and efficacy of tetracaine 1% and bupivacaine 0.75% in controlling pain following photorefractive keratectomy (PRK). *Eur J Ophthalmol.* 1997;7:327–333.
11. Corbett MC, Marshall J. Corneal haze after photorefractive keratectomy: a review of etiological mechanism and treatment options. *Lasers Light Ophthalmol.* 1996;7:173–196.
12. Camellin M. Laser epithelial keratomileusis with mitomycin C: indications and limits. *J Refract Surg.* 2004;20:S693–S698.
13. Bedei A, Marabotti A, Giannecchini I, et al. Photorefractive keratectomy in high myopic defects with or without intraoperative mitomycin C: 1-year results. *Eur J Ophthalmol.* 2006;16:229–234.
14. Thornton I, Xu M, Krueger RR. Comparison of standard (0.02%) and low dose (0.002%) mitomycin C in the prevention of corneal haze following surface ablation for myopia. *J Refract Surg.* 2008; 24:S68–S76.
15. Gambato C, Ghirlando A, Moretto E, Busato F, Midena E. Mitomycin C modulation of corneal wound healing after photorefractive keratectomy in highly myopic eyes. *Ophthalmology.* 2005;112:208–218.
16. Dougherty PJ, Hardten DR, Lindstrom RL. Corneoscleral melt after pterygium surgery using a single intraoperative application of mitomycin-C. *Cornea.* 1996;15:537–540.
17. Safianik B, Ben-Zion I, Garzozi HJ. Serious corneoscleral complications after pterygium excision with mitomycin C. *Br J Ophthalmol.* 2002;86:357–358.

18. Rubinfeld RS, Pfister RR, Stein RM, et al. Serious complications of topical mitomycin-C after pterygium surgery. *Ophthalmology.* 1992;99:1647–1654.
19. Wu KY, Hong SJ, Huang HT, Lin CP, Chen CW. Toxic effects of mitomycin-C on cultured corneal keratocytes and endothelial cells. *J Ocul Pharmacol Ther.* 1999;15:401–411.
20. Netto MV, Mohan RR, Sinha S, Sharma A, Gupta PC, Wilson SE. Effect of prophylactic and therapeutic mitomycin C on corneal apoptosis, cellular proliferation, haze, and long-term keratocyte density in rabbits. *J Refract Surg.* 2006;22:562–574.
21. Jester JV, Petroll WM, Cavanagh HD. Corneal stromal wound healing in refractive surgery: the role of myofibroblasts. *Prog Retin Eye Res.* 1999;18:311–356.
22. Netto MV, Mohan RR, Ambrósio R Jr, Hutcheon AE, Zieske JD, Wilson SE. Wound healing in the cornea: a review of refractive surgery complications and new prospects for therapy. *Cornea.* 2005;24:509–522.
23. Netto MV, Mohan RR, Sinha S, Sharma A, Dupps W, Wilson SE. Stromal haze, myofibroblasts, and surface irregularity after PRK. *Exp Eye Res.* 2006;82:788–797.
24. Mohan RR, Hutcheon AE, Choi R, et al. Apoptosis, necrosis, proliferation, and myofibroblast generation in the stroma following LASIK and PRK. *Exp Eye Res.* 2003;76:71–87.
25. Jester JV, Moller-Pedersen T, Huang J, et al. The cellular basis of corneal transparency: evidence for 'corneal crystallins'. *J Cell Sci.* 1999;112:613–622.
26. Tuominen IS, Tervo TM, Teppo AM, Valle TU, Grönhagen-Riska C, Vesaluoma MH. Human tear fluid PDGF-BB, TNF-α and TGF-β1 vs corneal haze and regeneration of corneal epithelium and subbasal nerve plexus after PRK. *Exp Eye Res.* 2001;72:631–641.
27. Vesaluoma M, Teppo AM, Grönhagen-Riska C, Tervo T. Platelet-derived growth factor-BB (PDGF-BB) in tear fluid: a potential modulator of corneal wound healing following photorefractive keratectomy. *Curr Eye Res.* 1997;16:825–831.
28. Vesaluoma M, Teppo AM, Grönhagen-Riska C, Tervo T. Increased release of tumour necrosis factor-α in human tear fluid after excimer laser induced corneal wound. *Br J Ophthalmol.* 1997;81:145–149.
29. Jester JV, Barry-Lane PA, Petroll WM, Olsen DR, Cavanagh HD. Inhibition of corneal fibrosis by topical application of blocking antibodies to TGF- beta in the rabbit. *Cornea.* 1997;16:177–187.
30. Saika S. TGF-beta signal transduction in corneal wound healing as a therapeutic target. *Cornea.* 2004;23:S25–S30.
31. Jester JV, Huang J, Petroll WM, Cavanagh HD. TGF-β induced myofibroblast differentiation of rabbit keratocytes requires synergistic TGF-β, PDGF and integrin signaling. *Exp Eye Res.* 2002;75:645–657.
32. Border WA, Noble NA. Transforming growth factor beta in tissue fibrosis. *N Engl J Med.* 1994;331:1286–1292.
33. Kume S, Haneda M, Kanasaki K, et al. SIRT1 inhibits transforming growth factor beta–induced apoptosis in glomerular mesangial cells via Smad7 deacetylation. *J Biol Chem.* 2007;282:151–158.
34. Glenisson W, Castronovo V, Waltregny D. Histone deacetylase 4 is required for TGF-β1–induced myofibroblastic differentiation. *Biochim Biophys Acta.* 2007;1773:1572–1582.
35. Struhl K. Histone acetylation and transcriptional regulatory mechanisms. *Genes Dev.* 1998;12:599–606.
36. Mottet D, Castronovo V. Histone deacetylases: target enzymes for cancer therapy. *Clin Exp Metast.* 2008;25:183–189.
37. Yoshida M, Kijima M, Akita M, Beppu T. Potent and specific inhibition of mammalian histone deacetylase both in vivo and in vitro by trichostatin A. *J Biol Chem.* 1990;265:17174–17179.
38. Niki T, Rombouts K, De Bleser P, et al. A histone deacetylase inhibitor, trichostatin A, suppresses myofibroblastic differentiation of rat hepatic stellate cells in primary culture. *Hepatology.* 1999;29:858–867.
39. Rombouts K, Niki T, Greenwel P, et al. Trichostatin A, a histone deacetylase inhibitor, suppresses collagen synthesis and prevents TGF-β1–induced fibrogenesis in skin fibroblasts. *Exp Cell Res.* 2002;278:184–197.
40. Ghosh AK, Mori Y, Dowling E, Varga J. Trichostatin A blocks TGF-beta–induced collagen gene expression in skin fibroblasts: involvement of Sp1. *Biochem Biophys Res Commun.* 2007;354:420–426.
41. Mohan RR, Mohan RR, Kim WJ, Wilson SE. Modulation of TNF-α–induced apoptosis in corneal fibroblasts by transcription factor NF-κB. *Invest Ophthalmol Vis Sci.* 2000;41:1327–1336.
42. Mohan RR, Kim WJ, Mohan RR, Chen L, Wilson SE. Bone morphogenic proteins 2 and 4 and their receptors in the adult human cornea. *Invest Ophthalmol Vis Sci.* 1998;39:2626–2636.
43. Fantes FE, Hanna KD, Waring GO, Pouliquen Y, Thompson KP, Savoldelli M. Wound healing after excimer laser keratomileusis (photorefractive keratectomy) in monkeys. *Arch Ophthalmol.* 1990;108:665–675.
44. Mohan RR, Stapleton WM, Sinha S, Netto MV, Wilson SE. A novel method for generating corneal haze in anterior stroma of the mouse eye with the excimer laser. *Exp Eye Res.* 2008;86:235–240.
45. Corbett MC, Prydal JI, Verma S, Oliver KM, Pande M, Marshall J. An in vivo investigation of the structures responsible for corneal haze after photorefractive keratectomy and their effect on visual function. *Ophthalmology.* 1996;103:1366–1380.
46. Moller-Pedersen T, Cavanagh HD, Petroll WM, Jester JV. Stromal wound healing explains refractive instability and haze development after photorefractive keratectomy: a 1-year confocal microscopic study. *Ophthalmology.* 2000;107:1235–1245.
47. Gray SG, Dangond F. Rationale for the use of histone deacetylase inhibitors as a dual therapeutic modality in multiple sclerosis. *Epigenetics.* 2006;1:67–75.
48. Kong Y, Tannous P, Lu G, et al. Suppression of class I and II histone deacetylases blunts pressure-overload cardiac hypertrophy. *Circulation.* 2006;113:2579–2588.
49. Hahnen E, Eyüpoglu IY, Brichta L, et al. In vitro and ex vivo evaluation of second-generation histone deacetylase inhibitors for the treatment of spinal muscular atrophy. *J Neurochem.* 2006;98:193–202.
50. Hautmann MB, Madsen CS, Owens GK. A transforming growth factor beta (TGF-beta) control element drives TGF- beta–induced stimulation of smooth muscle alpha-actin gene expression in concert with two CArG elements. *J Biol Chem.* 1997;272:10948–10956.
51. Ishikawa O, Yamakage A, LeRoy EC, Trojanowska M. Persistent effect of TGF-beta 1 on extracellular matrix gene expression in human dermal fibroblasts. *Biochem Biophys Res Commun.* 1990;169:232–238.
52. Van Lint C, Emiliani S, Verdin E. The expression of a small fraction of cellular genes is changed in response to histone hyperacetylation. *Gene Expr.* 1996;5:245–253.
53. Wilson SE, Mohan RR, Hong JW, Lee JS, Choi R, Mohan RR. The wound healing response after laser in situ keratomileusis and photorefractive keratectomy: elusive control of biological variability and effect on custom laser vision correction. *Arch Ophthalmol.* 2001;119:889–896.
54. Chen C, Michelini-Norris B, Stevens S, et al. Measurement of mRNAs for TGF-ss and extracellular matrix proteins in corneas of rats after PRK. *Invest Ophthalmol Vis Sci.* 2000;41:4108–4116.
55. Tuli SS, Liu R, Chen C, Blalock TD, Goldstein M, Schultz GS. Immunohistochemical localization of EGF, TGF-α, TGF-β, and their receptors in rat corneas during healing of excimer laser ablation. *Curr Eye Res.* 2006;31:709–719.
56. Møller-Pedersen T, Cavanagh HD, Petroll WM, Jester JV. Neutralizing antibody to TGF-β modulates stromal fibrosis but not regression of photoablative effect following PRK. *Curr Eye Res.* 1998;17:736–747.
57. Cordeiro MF, Mead A, Ali RR, et al. Novel antisense oligonucleotides targeting TGF-β inhibit in vivo scarring and improve surgical outcome. *Gene Ther.* 2003;10:59–71.
58. Duvic M, Vu J. Vorinostat in cutaneous T-cell lymphoma. *Drugs Today.* 2007;43:585–599.